Composites Research

Vol. 29, No. 6, 388-394 (2016)
DOI: http://dx.doi.org/10.7234/composres.2016.29.6.388
ISSN 2288-2103(Print), ISSN 2288-2111(Online)

Special Issue Paper

# Comparison of the Stress Concentration Factors for GFRP Plate having Centered Circular Hole by Three Resource-Conserving Methods

**Zhongchen Gao*, Soo-Jeong Park**, Yun-Hae Kim***†**

**ABSTRACT:** Fiber reinforced plastic (FRP) composites have drawn increasing attentions worldwide for decades due to its outstanding properties. Stress concentration factor (SCF) as an essential parameter in materials science are critically considered in structure design and application, strength assessment and failure prediction. However, investigation of stress concentration in FRP composites has been rarely reported so far. In this study, three resource-conserving analyses (Isotropic analysis, Orthotropic analysis and Finite element analysis) were introduced to plot the $K_T^A - d/W$ curve for E-glass/epoxy composite plate with the geometrical defect of circular hole placed centrally. The plates were loaded to uniaxial direction for simplification. Finite element analysis (FEA) was carried out via ACP (ANSYS composite prepost module). Based on the least squares method, a simple expression of fitting equation could be given based on the simulated results of a set of discrete points. Finally, all three achievable solutions were presented graphically for explicit comparison. In addition, the investigation into customized efficient SCFs has also been carried out for further reference.

**Key Words:** E-glass/epoxy composite plate, Circular hole, Stress concentration factor, FEA

## 1. INTRODUCTION

Recently, materials of the existing structure in industrial field such as aluminum and metal have been substituted for composite materials due the increased the needs for structural stabilities under rapid changes of temperature [1]. Most composite material structures include joint parts and this often results in reducing efficiency of whole structures. Especially mechanical joint is a way to selecting typically. In the practical application of composites, however, the riveted joints have inevitably holes, which cause stress concentration.

However, stress concentrations around holes will have great influence on the performance of the structure. The failure strengths of composite materials are strongly sensitive to hole. The net failure stress, which takes into account the reduction in cross-sectional area, is typically much less than the ultimate tensile strength of the same materials without the hole. For example, strength reduction of 40-60% has been reported for a glass fiber reinforced plastic plate [2].

In this study, we consider the stress concentration factor (SCF), $K_T^A$ in nonrestrictive stress concentration situation--with finite width or considerable $d/W$ scale. $K_T^A$ is defined as the ratio of the maximum stress in the presence of a geometric irregularity or discontinuity to the stress that would exist at the same point if the irregularity was not present [3].

## 2. THEORETICAL ANALYSES

### 2.1 Isotropic Analysis

Currently, most of the strength analysis associated with SCFs are based on the condition of infinite width/diameter plate because it has a closed form solution of stress distributions. In the case of infinite width plate under uniaxial tension (Fig. 1) $\sigma_y$ in the 1-axis direction at the point on the 2-axis in front of the hole may be approximated by equations (1) and (2) [4]:

Received 1 December 2016, received in revised form 27 December 2016, accepted 29 December 2016

*College of Engineering, Seoul National University
**Department of Material Engineering, Graduate School, Korea Maritime and Ocean University
***†Department of Mechanical Engineering, Korea Maritime and Ocean University, Corresponding author (E-mail: yunheak@kmou.ac.kr)

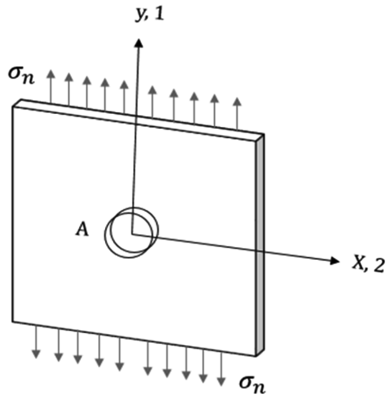


**Fig. 1.** Plate with a circular hole and under uniaxial tension

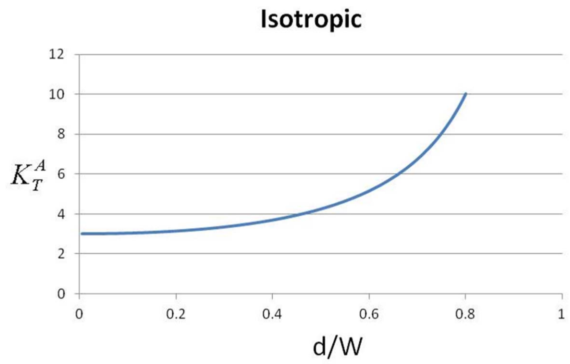


**Fig. 2.** The SCFs at point A for isotropic plate under uniaxial tension

$$\sigma_{y(x,0)} = \sigma_n\left(1+0.5\frac{\rho^2}{x^2}+1.5\frac{\rho^4}{x^4}\right) \tag{1}$$

$$K_{T,i}^{\infty,A} = \frac{\sigma_y(\rho,0)}{\sigma_n} = 3,\ (x=\rho) \tag{2}$$

$\sigma_{y(x,0)}$ : Stress along y direction at the coordinate of $(x, 0)$; ρ: Radius of the hole.

Due to the considerably small $d/W$ ratio in most practical applications, it is necessary to take into account the effect of finite width/diameter on SCFs. By defining a scale factor as the ratio of the finite width to the infinite width, such effect can be suitably considered.

By using a curve fitting technique, the SFs for an isotropic plate with a centered hole can be determined accurately [5,6]:

$$\frac{K_{T,i}^{\infty,A}}{K_{T,i}^{A}} = \frac{3(1-d/W)}{2+(1-d/W)^3} \tag{3}$$

where $K_{T,i}^{\infty,A}$ and $K_{T,i}^{A}$ represent the SCFs at point $A$ in an isotropic plate under uniaxial tension with infinite and finite width, respectively. The $d$ is the diameter of the hole and $W$ is the width of the plate. ∞ represents infinite width plate.

According to equation (2) and (3), an $K_{T,i}^{A}$ can be simply expressed as:

$$K_{T,i}^{A} = (1-d/W)^2+2/(1-d/W) \tag{4}$$

From above analysis, it can be known that the SCFs at point A is not a function of the material properties. With a same value of the $d/W$, there is exactly the same value of $K_{T,i}^{A}$. The $d/W$ is the only variable to the $K_{T,i}^{A}$. As is well known, for isotropic materials, which lies in linear elastic region, the stress distribution is only a function of geometry and force. Since the behavior of fully solidified epoxy is roughly linear and elastic, the above analysis is appropriate. Therefore, here we plot the $K_T^A - d/W$ curve, as shown in Fig. 2.

**2.2 Orthotropic Analysis**

The stress-strain relation for a three dimensional linear elastic, anisotropic material is given as:

$$\{\sigma\} = [C]\{\varepsilon\} \tag{5}$$

which is also known as Hooke's law. $\sigma$ and $\varepsilon$ are stress and strain vectors respectively. The matrix of $[C]$ is referred to as the material stiffness matrix which has 21 independent constants.

In the case of an orthotropic plate, it can be simplified as:

$$\begin{Bmatrix}\sigma_1\\ \sigma_2\\ \tau_{12}\end{Bmatrix} = \begin{bmatrix}Q_{11} & Q_{12} & 0\\ Q_{12} & Q_{22} & 0\\ 0 & 0 & Q_{66}\end{bmatrix}\begin{Bmatrix}\varepsilon_1\\ \varepsilon_2\\ \gamma_{12}\end{Bmatrix} \tag{6}$$

Here, direction 1, 2 are the principal material axes.

The coefficient of the stiffness matrix $Q$ are expressed as following:

$$Q_{11} = E_{11}/(1-\nu_{11}\nu_{21})$$

$$Q_{22} = E_{22}/(1-\nu_{12}\nu_{21})$$

$$Q_{12} = \nu_{21}E_{11}/(1-\nu_{12}\nu_{21})$$

$$Q_{66} = G_{12} \tag{7}$$

Only four of five engineering elastic constants are independent. The fifth one could be derived by:

$$E_{11}\nu_{21} = E_{22}\nu_{12} \tag{8}$$

For an infinite orthotropic plate containing a circular hole under to a remote uniform stress $\sigma_n$ in direction 1 (Fig. 3), with assumption of linear-elastic response, the normal stress $\sigma_y$ in the 1-axis direction at the point on the 2-axis in front of the hole can be approximated by [7]:

$$\sigma_y(x,0) = \frac{\sigma_n}{2}\left\{2+\left(\frac{d}{2x}\right)^2+3\left(\frac{d}{2x}\right)^4-(1+n-3)\left[5\left(\frac{d}{2x}\right)^6-7\left(\frac{d}{2x}\right)^8\right]\right\}$$

$$(2x>d) \tag{9}$$

$$n=\sqrt{2\left(\frac{E_{11}}{E_{22}}-v_{12}\right)+\frac{E_{11}}{G_{12}}} \tag{10}$$

Therefore, the SCF of point A, ($x = a$), $K_T^{\infty,A}$ is:

$$K_T^{\infty,A}=1+n=1+\sqrt{2\left(\frac{E_{11}}{E_{22}}-v_{12}\right)+\frac{E_{11}}{G_{12}}} \tag{11}$$

*E, v, G* could be measured by an experiment method.

Equation (10) gives a constant value of the $K_T^{\infty,A}$ for the same material regardless of the circular hole size. As for the finite orthotropic laminates, a closed form solution, the finite-width correction (FWC) factor has been derived based on an approximate stress analysis [8,9]:

$$\frac{K_T^{\infty,A}}{K_T^A}=\frac{3(1-d/W)}{2+(1-d/W)^3}+\frac{1}{2}\left(\frac{d}{W}M\right)^6(K_T^{\infty,A}-3)\left[1-\left(\frac{d}{W}M\right)^2\right] \tag{12}$$

where $K_T^{\infty,A}$ and the $K_T^A$ represent the SCF at point $A$ for an orthotropic plate under uniaxial tension with infinite and finite width, respectively.

$M$ is a magnification factor, which is only a function of $d/W$. The detailed expression is given as [9]:

$$M=\sqrt{\frac{-1+\sqrt{1-8\left[\frac{3(1-d/W)}{2+(1-d/W)^3}-1\right]}}{2(d/W)^2}} \tag{13}$$

Obviously, at a certain value of the $d/W$, the SCFs only depend on the orthotropic properties. In this paper, the composite plate is designed to have the balanced and symmetry stacking sequence of [0/90/0/90]s which is representative in real application (Fig. 3). Based on the experimental measurement, the relevant orthotropic material parameters in average are tabulated below.

The shear modulus $G_{12}$ is computed by [10]:

$$\frac{1}{G_{12}}=\frac{4}{E_{45}}-\frac{1-2v_{12}}{E_{11}}-\frac{1}{E_{22}} \tag{14}$$

Equation (14) indicates that in addition to $E_{11}$, $E_{22}$ and $v_{12}$, require Young's modulus in 45 degree direction $E_{45}$ is required, which equals to 13.16 GPa. According to equation (11), (12), (13), the $K_T^A - d/W$ function based on orthotropic analysis has been determined by substituting the orthotropic elasticity properties in Table 1. The curve is plotted in Fig. 4:

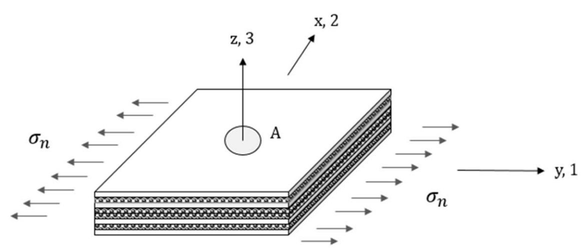


**Fig. 3.** Designed fiber reinforced cross-ply composite plate in [0/90/0/90]s layups with circular hole

**Table 1.** The orthotropic material parameters of E-glass-epoxy [0/90/0/90]s plate

| $E_{11}$ (GPa) | $E_{22}$ (GPa) | $V_{12}$ | $G_{12}$ (GPa) |
|---|---|---|---|
| 21.1 | 20.3 | 0.379 | 4.11 |

$E_{11}$, $E_{22}$: modulus in two principal material axes; $V_{12}$: Poisson's ratio; $G_{12}$: shear modulus.

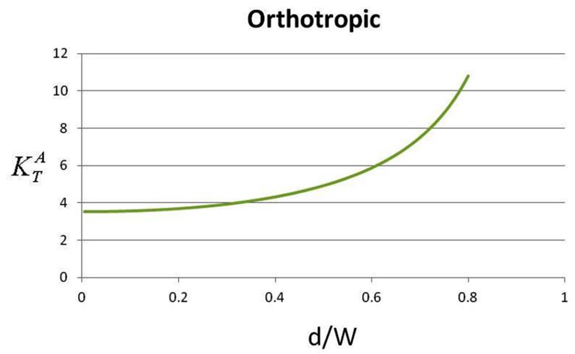


**Fig. 4.** The SCFs at point A for E-glass-epoxy plate with a circular hole under uniaxial tension by orthotropic analysis (in $E_{11}$ direction)

### 2.3 FEA Simulation

Via ACP module in ANSYS-Workbench, various models with all difference in shape, thickness, orientation, could be simulated only with an essential condition of the orthotropic elasticity of one single ply. It provides an efficient pathway and brings huge convenience to the estimation to SCFs.

According to experimental results, the least required orthotropic material parameters are listed in Table 2.

The $v_{23}$ is suggested as the value of Poisson's ratio in pure epoxy bulk. The $G_{23}$ is calculated by $G_{23}=E_{22}/2(1+v_{23})$ [11].

The geometry (Fig. 3) is designed to be rectangle plate with a central circular hole. For the same $d/W$, the actual hole size or plate width has little influence on the SCFs [12]. All composite plates are fixed with the same width, thickness and length, which are 20 mm, 3.6 mm and 200 mm, respectively. The hole diameter is the only variable (Table 3). In addition, the layup structure is demonstrated in Fig. 5 as well as polar properties.

In order to ensure the accuracy for solution, the element size is adjusted to as small as 0.0005 m. There are two behaviors for meshing hard and soft. If we choose the hard option for edges,

**Table 2.** Orthotropic material parameters of single UD-E-glass/epoxy plate

| | | | | | |
|---|---|---|---|---|---|
| $E_{11}$ (GPa) | 41.9 | $V_{12}$ | 0.3254 | $G_{12}$ (GPa) | 3.4 |
| $E_{22}$ (GPa) | 7.8 | $V_{23}$ | 0.4034 | $G_{23}$ (GPa) | 2.8 |
| $E_{33}$ (GPa) | 7.8 | $V_{13}$ | 0.3254 | $G_{13}$ (GPa) | 3.4 |

$E_{11}$, $E_{22}$, $v_{12}$, $G_{12}$: refer to the Table 1; $E_{33}$: modulus in the perpendicular direction; $v_{23}$, $v_{13}$: Poisson's ratio; $G_{23}$, $G_{13}$: shear modulus.

**Table 3.** Geometrical sizes of the plates

| d (mm) | 2 | 3 | 4 | 5 | 6 | 7 | 8 | 9 |
|---|---|---|---|---|---|---|---|---|
| Length | 200 | 200 | 200 | 200 | 200 | 200 | 200 | 200 |
| Thickness | 3.6 | 3.6 | 3.6 | 3.6 | 3.6 | 3.6 | 3.6 | 3.6 |
| Width | 20 | 20 | 20 | 20 | 20 | 20 | 20 | 20 |
| $d/W$ | 0.1 | 0.15 | 0.2 | 0.25 | 0.3 | 0.35 | 0.4 | 0.45 |
| d (mm) | 10 | 11 | 12 | 13 | 14 | 15 | 16 | |
| Length | 200 | 200 | 200 | 200 | 200 | 200 | 200 | |
| Thickness | 3.6 | 3.6 | 3.6 | 3.6 | 3.6 | 3.6 | 3.6 | |
| Width | 20 | 20 | 20 | 20 | 20 | 20 | 20 | |
| $d/W$ | 0.5 | 0.55 | 0.6 | 0.65 | 0.7 | 0.75 | 0.8 | |

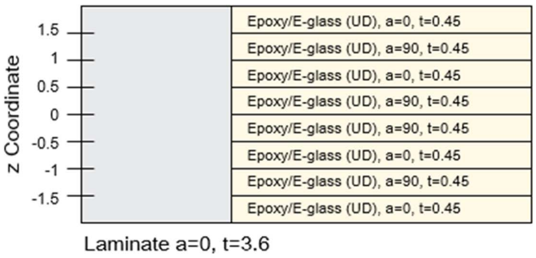


**(a) Laminate. MP, AP**

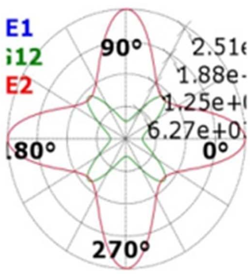


**(b) Polar properties**

**Fig. 5.** Layup and polar properties

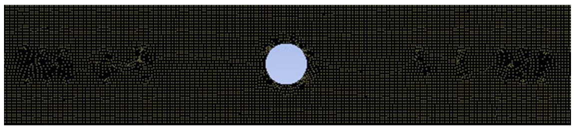

**Fig. 6.** FEA mesh for 7/20-*d/W* scale plate

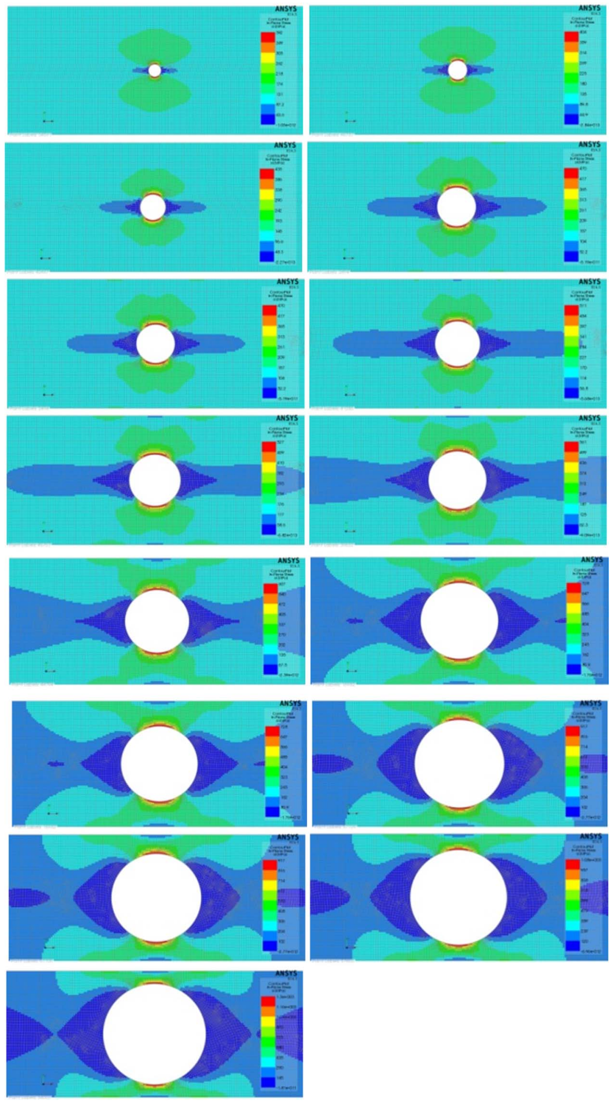

**Fig. 7.** Stress in 1-axis direction Nephogram with different *d/W* scale

the size or number of divisions is fixed on the edge and cannot be changed by the meshing algorithm and the likelihood of a mesh failure increases. On the other hand, if we chow the soft option for edges, faces and bodies, the size control will be affected by proximity, curvature and local remeshing during the meshing process. Finally, meshing is generated in hard behavior to guarantee, the meshing size will not be affected by curvature, as shown in Fig. 6:

Since it is all about stress distribution, the input load is irrelevant. In any case, the solution reveals a significant effect of repeated stress concentration along larger diameter (Fig. 7).

The discrete values of the $K_T^A$ (Table 4) were extracted to plot the $K_T^A$–$d/W$ curve. Accordingly, the process variables of the system are fitted by polynomial least square method in MATLAB. The following curve has been produced, as shown

**Table 4.** SCFs at point A with different *d/W* scale in arithmetic sequence

| $d/W$ | 0.1 | 0.15 | 0.2 | 0.25 | 0.3 |
|---|---|---|---|---|---|
| $K_T^A$ | 3.079 | 3.173 | 3.285 | 3.462 | 3.658 |
| $d/W$ | 0.35 | 0.4 | 0.45 | 0.5 | 0.55 |
| $K_T^A$ | 3.858 | 4.118 | 4.395 | 4.708 | 5.153 |
| $d/W$ | 0.6 | 0.65 | 0.7 | 0.75 | 0.8 |
| $K_T^A$ | 5.693 | 6.325 | 7.196 | 8.44 | 10.221 |

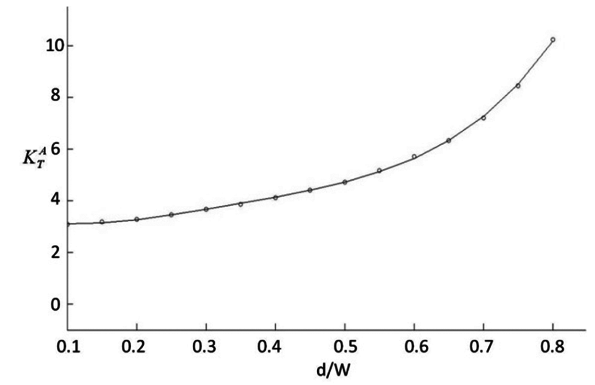


**Fig. 8.** Fitted curve of $K_T^A$ –*d/W* produced by MATLAB

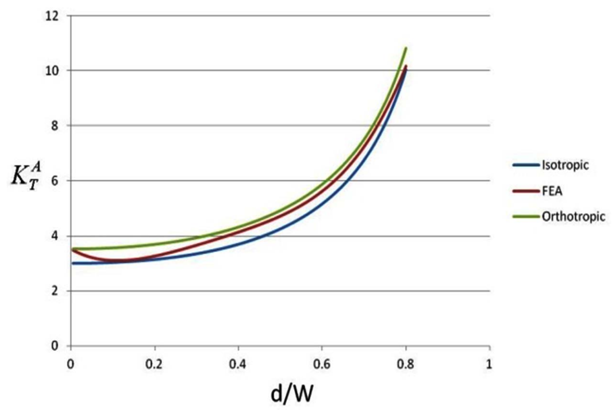


**Fig. 9.** $K_T^A$ –*d/W* curves under axial tension

in Fig. 8.

In addition, the approximate equation in polynomial form is expressed:

$$K_T^A\left(\frac{d}{W}\right) = 77.0567\left(\frac{d}{W}\right)^4 - 103.2063\left(\frac{d}{W}\right)^3 + 54.4874\left(\frac{d}{W}\right)^2 - 8.6833\left(\frac{d}{W}\right) + 3.5266 \quad (15)$$

In this equation, one of the minimal extremum points is located around $d/W = 0.11$. Therefore, only [0.11, 1] of the $d/W$ can be taken into account. In consideration of real application in engineering, the reasonable interval of the $d/W$ could be set as [0.1, 0.8].

## 3. COMPARISON

Based on the research above, all three analyses emphasize the considerable $d/W$ scale effect on the SCF. Each solution reveals an increment greater than 7 on the SCFs of point A in between 0.1 and 0.8 of the $d/W$ (Table 5).

As shown in Fig. 9, three curves roughly in parallel with each other, and each $K_T^A$ increases progressively with the $d/W$ in [0.1,0.8] interval. Among them, the values of $K_T^A$ from orthotropic solution are relatively large, and the $K_T^A$ in isotropic situation are small in contrary. The $K_T^A$ from FEA solution varies in between orthotropic curve and isotropic curve. Under the same tendency (Fig. 9), there are several significant differences among them. Isotropic solution is dependent on material properties and the geometry. However, orthotropic solution and FEA solution are closely related to the orthotropic elasticity. Consequently, the accurate solution to the problem is necessary. For orthotropic solution, 4 independent parameters are required in the investigation of imperforated plate. On the other hand, FEA solution needs 9 elastic material parameters of one single ply (Table 2). The suitable approach to choose depends on what properties of the material we have previously obtained.

**Table 5.** Comparison of $K_T^A$ on each discrete value of *d/W*

| $d/W$ | 0.1 | 0.15 | 0.2 | 0.25 | 0.3 |
|---|---|---|---|---|---|
| $K_{T,I}^A$ | 3.032 | 3.075 | 3.14 | 3.229 | 3.347 |
| $K_{T,F}^A$ | 3.108 | 3.141 | 3.267 | 3.450 | 3.663 |
| $K_{T,O}^A$ | 3.572 | 3.623 | 3.698 | 3.802 | 3.938 |
| $d/W$ | 0.35 | 0.4 | 0.45 | 0.5 | 0.55 |
| $K_{T,I}^A$ | 3.499 | 3.693 | 3.939 | 4.25 | 4.646 |
| $K_{T,F}^A$ | 3.894 | 4.139 | 4.408 | 4.722 | 5.113 |
| $K_{T,O}^A$ | 4.110 | 4.326 | 4.594 | 4.928 | 5.347 |
| $d/W$ | 0.6 | 0.65 | 0.7 | 0.75 | 0.8 |
| $K_{T,I}^A$ | 5.16 | 5.837 | 6.757 | 8.061 | 10.04 |
| $K_{T,F}^A$ | 5.626 | 6.315 | 7.249 | 8.504 | 10.173 |
| $K_{T,O}^A$ | 5.881 | 6.577 | 7.513 | 8.833 | 10.822 |

I represents isotropic analysis; F represents FEA analysis; O represents orthotropic analysis.

## 4. EXPERIMENTAL RESULTS

In engineering, to predict the strength of a structure, an effective SCF is more referable, due to the variety of material properties, surface states, and structure sizes, etc. Here, we define the concept of effective SCF, $K_T'$ in the model of a plate with a circular hole:

$$K_T' = \frac{P}{P'} \quad (16)$$

where $P'$, $P$ are the limit loads of finite width plates with and without a circular hole, respectively.

Furthermore, SCF sensitivity coefficient $q$ has been introduced to indicate the influence of SCF on the actual strength performance:

$$q = \frac{(K_T' - 1)}{(K_T^A - 1)} \quad (17)$$

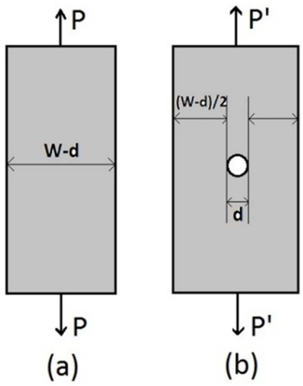


**Fig. 10.** Plates with and without a circular hole

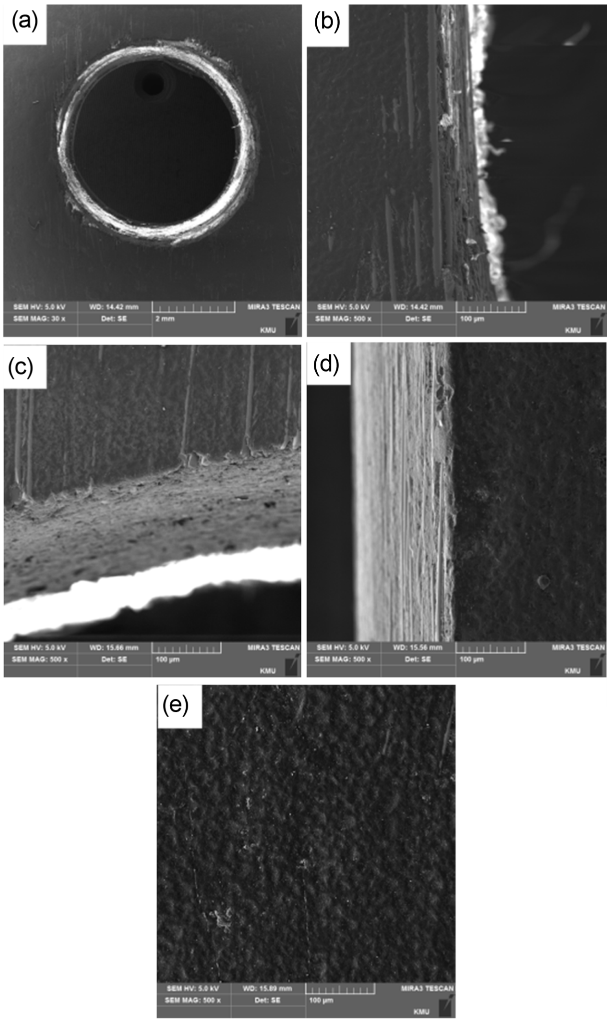


**Fig. 11.** Qualified condition of outside surface in center-perforated coupon

The sensitivity coefficient, $q$, equals to zero means that there is no influence of SCF on the strength performance. Inversely, $q = 1$ stands for the tremendous reduction on the strength caused by SCF.

By conducting a contrast tension test between virgin plates and perforated plates (Fig. 10), the series of values for $K_T'$ could be calculated. The width $W$ and length $L$ of plates are summarized in Table 3.

In this study, all centered holes in plates were generated using common drilling machine. After holes were drilled, the specimens were examined using SEM. In order to enhance the image, the outside surface was coated with platinum. Only the specimens in a sound condition, which has smooth surface with evenly covered resin (Fig. 11-(e)) and shows no cracks around hole areas (Fig. 11-(a), (b), (c)) and edge regions (Fig. 11-(d)), were selected for the tension test.

All specimens were incrementally loaded in universal testing machine with displacement rate of 0.5 mm/min. Finally, 12 sets of effective SCF data were collected in [0.1, 0.65] interval of $d/W$. Averages are tabulated down below (Table 6).

The effective SCF is increasing with increasing of d as expected. However, the values are confined to be less than 1.25 up to $d/W = 0.65$. The SCF sensitivity coefficients have been computed from equation (17), and summarized in Table 7. The computation shows no increasing or declining trend whatsoever, and the values vary in typical fluctuating behavior which mainly caused by measurement errors. The means values of $q_I$, $q_F$ and $q_O$ are 4.98%, 4.49% and 4.06%, respectively. Such small values of q predict small reduction in the strength performance of the structure and verify the fact of significant enhancement due to the existence of glass fibers inside epoxy matrix as reported in many studies. According to the previous researches, the low percentage of SCF sensitivity coefficient is mainly the result of crack resistance behavior of fibers. However, the effect of stress redistribution caused by the universal vertical crack found in the later loading process (Fig. 12) may have further influence on the q value. In order to explain this, further investigation will be necessary.

**Table 6.** Effective SCF at certain *d/W*

| $d/W$ | 0.105 | 0.16 | 0.2 | 0.2505 | 0.3 | 0.35 |
|---|---|---|---|---|---|---|
| ESCF | 1.0984 | 1.1093 | 1.1083 | 1.1163 | 1.1243 | 1.1257 |
| $d/W$ | 0.4 | 0.44 | 0.485 | 0.54 | 0.6 | 0.65 |
| ESCF | 1.1395 | 1.1418 | 1.1482 | 1.1611 | 1.1934 | 1.2475 |

**Table 7.** SCF sensitivity coefficients

| $q$ \ $d/W$ | 0.105 | 0.16 | 0.2 | 0.2505 | 0.3 | 0.35 |
|---|---|---|---|---|---|---|
| $q_{I\,(\%)}$ | 4.83 | 5.24 | 5.06 | 5.22 | 5.29 | 5.03 |
| $q_{F\,(\%)}$ | 4.67 | 5.06 | 4.78 | 4.75 | 4.67 | 4.35 |
| $q_{O\,(\%)}$ | 3.82 | 4.15 | 4.01 | 4.15 | 4.23 | 4.04 |
| $q$ \ $d/W$ | 0.4 | 0.44 | 0.485 | 0.54 | 0.6 | 0.65 |
| $q_{I\,(\%)}$ | 5.18 | 4.92 | 4.71 | 4.53 | 4.65 | 5.12 |
| $q_{F\,(\%)}$ | 4.44 | 4.23 | 4.09 | 4.00 | 4.18 | 4.66 |
| $q_{O\,(\%)}$ | 4.19 | 4.01 | 3.88 | 3.79 | 3.96 | 4.44 |

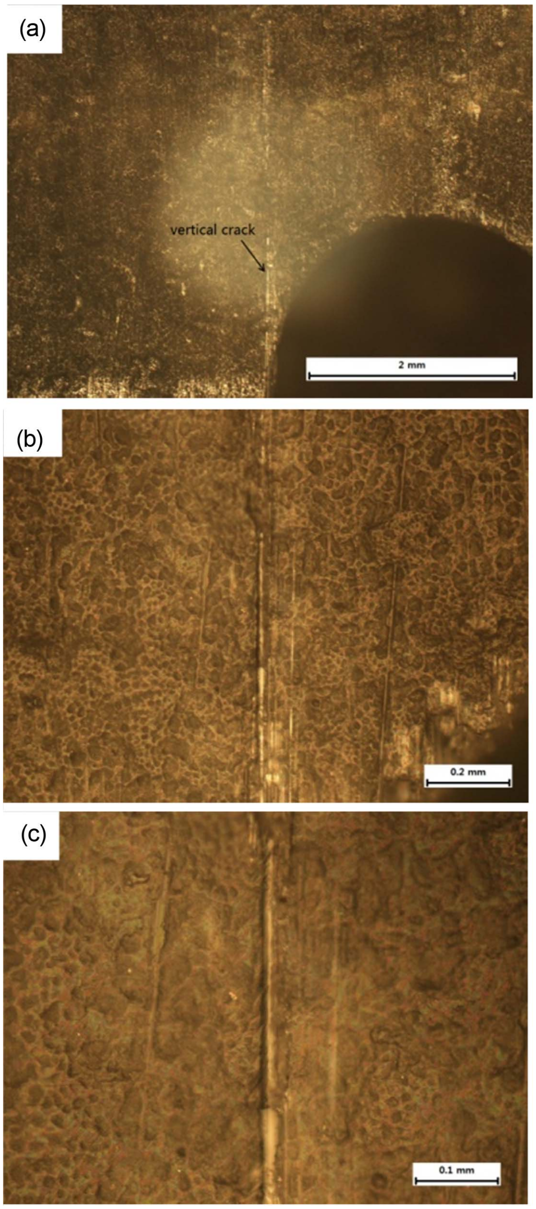


**Fig. 12.** Vertical cracks found right in the vicinity of hole edge at later stage of loading process

## 4. CONCLUSIONS

In this study, three theoretical methods have been carried out to estimate $K_T^A$ with the variation of $d/W$ in an E-glass/epoxy composite plate having a central circular hole. The analytic results calculated by orthotropic method are larger than the ones calculated by FEA simulation. The $d/W$ values are in the range between 0.1 and 0.8. Since the isotropic analysis is independent from material properties, it's less referable. Instead of searching for appropriate failure criterion [13,14], an empirical relation is preferred to predict the actual failure. The SCF sensitivity coefficient calculated FEA solution in [0.1, 0.65] interval of the $d/W$ is 4.49, which is larger than the value of 4.06 calculated from orthotropic solution. The subject of this study aims is to provide simple and efficient ways for the estimation of the hole effect on the plate structure. The proper method is largely dependent on the known conditions. The vertical crack found in tension test needs further investigation.

## ACKNOWLEDGEMENT

This work was supported by the Korean Small Business Innovation Research Program and Research Institute funded Korea Small and Medium Business Administration in 2016 under Grant number S2328725.

## REFERENCES

1. Cho, H.K., Seo, J.K., Kim, J.B., Jang, T.S., Cha, W.H., Lee, D.G., and Myung, N.H., "Development of a Composite Spacecraft Structure for STSAT-3 Satellite Program", *Journal of the Korean Society for Aeronautical and Space Sciences*, Vol. 38, No. 7, 2010, pp. 727-736.
2. Adams, K.M., *The Effect of Cutouts on Strength of GRP for Naval Ship Hulls*, Master Thesis, Institutional Archive of the Naval Postgraduate School, USA, 1986.
3. Gao, Z., *Study on the Theoretical SCFs and Effective SCFs for E-glass/Epoxy Composite Plate with Centered Circular Hole*, Master Thesis, Korea Maritime and Ocean University, Korea, 2014.
4. Sichuan University, *Manual for Stress Concentration Factor*, Senior Education Press, China, 1990.
5. Heywood, R.B., *Designing by photoelasticity*, Chapman and Hall, UK, 1952.
6. Brown, Jr., W.F., and Srawley, J.E., "Plane Strain Crack Toughness Testing of High Strength Metallic Materials", *American Society for Testing and Materials*, ASTM STP 410, 1966.
7. Lekhnistskii's, G., Tsai, W.S., and Cheron, T., *Anisotropic Plates*, Gordon and Breach Science Publishers, New York, 1968.
8. Tan, S.C., "Laminated Composites Containing an Elliptical Opening. I. Approximate Stress Analyses and Fracture Models", *Materials Science*, Vol. 21, No. 10, 1987, pp. 925-948.
9. Tan, S.C., *Stress Concentrations in Laminated Composites*, CRC Press, USA, 1994.
10. Rowlands, R.E., Daniel, I.M., and Whiteside, J.B., "Stress and Failure Analysis of a Glass-Epoxy Composite Plate with a Circular Hole", *Experimental Mechanics*, Vol. 13, No. 1, 1973, pp. 31-37.
11. Wang, J.X., "On a Constant in Elastostatic Problems for a Transversely Isotropic Body in the Plane of Isotropy", *Acta Metallurgica Sinica*, Vol. 17, No. 3, 2000, pp. 83-86.
12. Wu, H.C., and Mu, B., "On Stress Concentrations for Isotropic/Orthotropic Plates and Cylinders with a Circular Hole", *Composites Part B Engineering*, Vol. 34, No. 2, 2003.
13. Whitney, J.M., and Nuismer, R.J., "Stress Fracture Criteria for Laminated Composites Containing Stress Concentrations", *Materials Science*, Vol. 8, No. 3, 1974, pp. 253-265.
14. Nuismer, R.J., and Whitney, J.M., *Uniaxial Failure of Composite Laminates Containing Stress Concentrations*, ASTM International, USA, 1975.